Sponge contribution to the silicon cycle of a diatom-rich shallow bay

María López-Acosta[1*], Manuel Maldonado[2], Jacques Grall[3], Axel Ehrhold[4], Cèlia Sitjà[2], Cristina Galobart[2], Aude Leynaert[5]

[1] Oceanology Group, Instituto de Investigaciones Marinas (IIM-CSIC), C/ Eduardo Cabello 6, 36208 Vigo, Spain

[2] Department of Marine Ecology, Centro de Estudios Avanzados de Blanes (CEAB-CSIC), Acceso Cala St. Francesc 14, Blanes 17300, Girona, Spain

[3] Observatoire des Sciences de l'Univers, UMS 3113, Institut Universitaire Européen de la Mer, Technopôle Brest-Iroise, Plouzané 29280, France

[4] IFREMER, Géosciences Marines, Centre de Brest, BP70, CS10070, Plouzané 29280, France

[5] Laboratoire des Sciences de l'Environnement Marin, UMR 6539, Institut Universitaire Européen de la Mer, Technopôle Brest-Iroise, Plouzané 29280, France

*** Correspondence:**

María López-Acosta

lopezacosta@iim.csic.es

Running title: Coastal silicon cycle through sponges

Keywords: silicon, silicifiers, sponges, coastal ocean, benthic-pelagic coupling

Abstract

In coastal systems, planktonic and benthic silicifiers compete for the pool of dissolved silicon, a nutrient required to make their skeletons. The contribution of planktonic diatoms to the cycling of silicon in coastal systems is often well characterized, while that of benthic silicifiers such as sponges has rarely been quantified. Herein, silicon fluxes and stocks are quantified for the sponge fauna in the benthic communities of the Bay of Brest (France). A total of 45 siliceous sponge species living in the Bay account for a silicon standing stock of 1215 tons, while that of diatoms is only 27 tons. The silicon reservoir accumulated as sponge skeletons in the superficial sediments of the Bay rises to 1775 tons, while that of diatom skeletons is only 248 tons. These comparatively large stocks of sponge silicon were estimated to cycle two orders of magnitude slower than the diatom stocks. Sponge silicon stocks need years to decades to be renewed, while diatom turnover lasts only days. Although the sponge monitoring over the last 6 years indicates no major changes of the sponge stocks, our results do not allow to conclude if the silicon sponge budget of the Bay is at steady state, and potential scenarios are discussed. The findings buttress the idea that sponges and diatoms play contrasting roles in the marine silicon cycle. The budgets of these silicon major users need to be integrated and their connections revealed, if we aim to reach a full understanding of the silicon cycling in coastal ecosystems.

Introduction

There is great interest in understanding the cycling of silicon (Si) in marine environments because this nutrient is key to the functioning of marine ecosystems. In coastal oceans, Si is responsible for sustaining a large proportion of primary productivity and many of the food webs that ultimately sustain fish and human populations (Kristiansen and Hoell 2002; Ragueneau et al. 2006). Shortage of Si availability in coastal areas frequently reflects situations of ecosystem disequilibrium and proliferation of harmful algal blooms (Davidson et al. 2014; Glibert and Burford 2017; Thorel et al. 2017). Thus, a thorough understanding of the cycling of Si in coastal marine environments is critical for effective ecosystem management.

A substantial part of the Si cycling in the marine environment occurs through a variety of micro- and macro-organisms, the silicifiers, which require Si to build their siliceous skeletons (DeMaster 2003; Tréguer et al. 2021). To date, our understanding of the biogeochemical cycling of Si in the marine environment is based predominantly on the role of diatoms, microscopic unicellular eukaryotic algae which are the most abundant silicifiers in the global ocean (Malviya et al. 2016; Tréguer et al. 2021). Other silicifiers, such as siliceous Rhizaria and sponges, have received less attention and, consequently, their role is largely dismissed in most budgets of the marine Si cycle. To quantify the cycle contribution of siliceous sponges is particularly complicated given their benthic nature and heterogeneous distribution across the depths of the world's oceans. However, there is growing evidence that sponges are important contributors to the Si cycle in terms of Si standing stocks and reservoirs (Maldonado et al. 2010, 2019).

In the present study, the Bay of Brest (France) was monitored to assess the relative contribution of siliceous sponges to the Si budget of this emblematic coastal system. This Bay has been the subject of numerous ecological, biogeochemical, and physical studies and is currently one of the best-studied

coastal ecosystems in Europe, in terms of both structure and ecosystem functioning (Le Pape et al. 1996; Del Amo et al. 1997; Chauvaud et al. 2000; Ragueneau et al. 2018). In this ecosystem, diatoms dominate the annual pelagic primary production (Quéguiner and Tréguer 1984; Del Amo et al. 1997). Other planktonic silicifiers such as silicoflagellates, polycystines, and phaeodarians are rarely recorded in the monthly surveys of the planktonic community of the Bay, and when found, they are low abundant (https://www.phytobs.fr/). Silicic acid (dSi) concentrations vary over the year cycle from below 1 µM in spring and early summer up to 15-20 µM in late autumn and winter. Therefore, in this ecosystem diatom's activity is limited by dSi principally during spring and early summer (Ragueneau et al. 2002), but sponges are limited all year round, as these organisms need dSi concentrations of 100-200 µM to reach their maximum speed of Si consumption (K_M = 30-100 µM Si; Reincke and Barthel 1997; Maldonado et al. 2011, 2020; López-Acosta et al. 2016, 2018).

In this system, both dredging and diving research activities have identified important populations of siliceous sponges (Jean 1994; López-Acosta et al. 2018), and a previous study firstly estimated that the sponge silica production represents ca. 8% of the net annual silica production in the Bay (López-Acosta et al. 2018). Nevertheless, the large amounts of Si within the sponge bodies (i.e., the Si standing stock) remain unquantified, as well as the fate of such Si once the sponges die. Herein, we are estimating these parameters and providing the most complete cycle of Si through sponges for this coastal ecosystem. The findings are discussed within the regional Si budget of the Bay of Brest previously published by Ragueneau et al. (2005), which considered only the contribution of planktonic diatoms.

Materials

Study area

The Bay of Brest (NW France) is a semi-enclosed marine ecosystem of about 130 km^2 (harbors and estuaries not included) that is connected to the Atlantic Ocean through a narrow (1.8 km wide) and deep (45 m) strait. The Bay is a shallow system, with a maximum depth of 40 m and a mean depth of 8 m. It is a macro-tidal (maximum tidal amplitude = 8 m) system that receives high nutrient loadings mainly from two small rivers (Fig. 1a). During all the year cycle, the tidal and wind currents together with the shallowness of the Bay make nutrient concentration to remain relatively homogeneous in the water column (Delmas and Tréguer 1985; Salomon and Breton 1991; Le Pape et al. 1996).

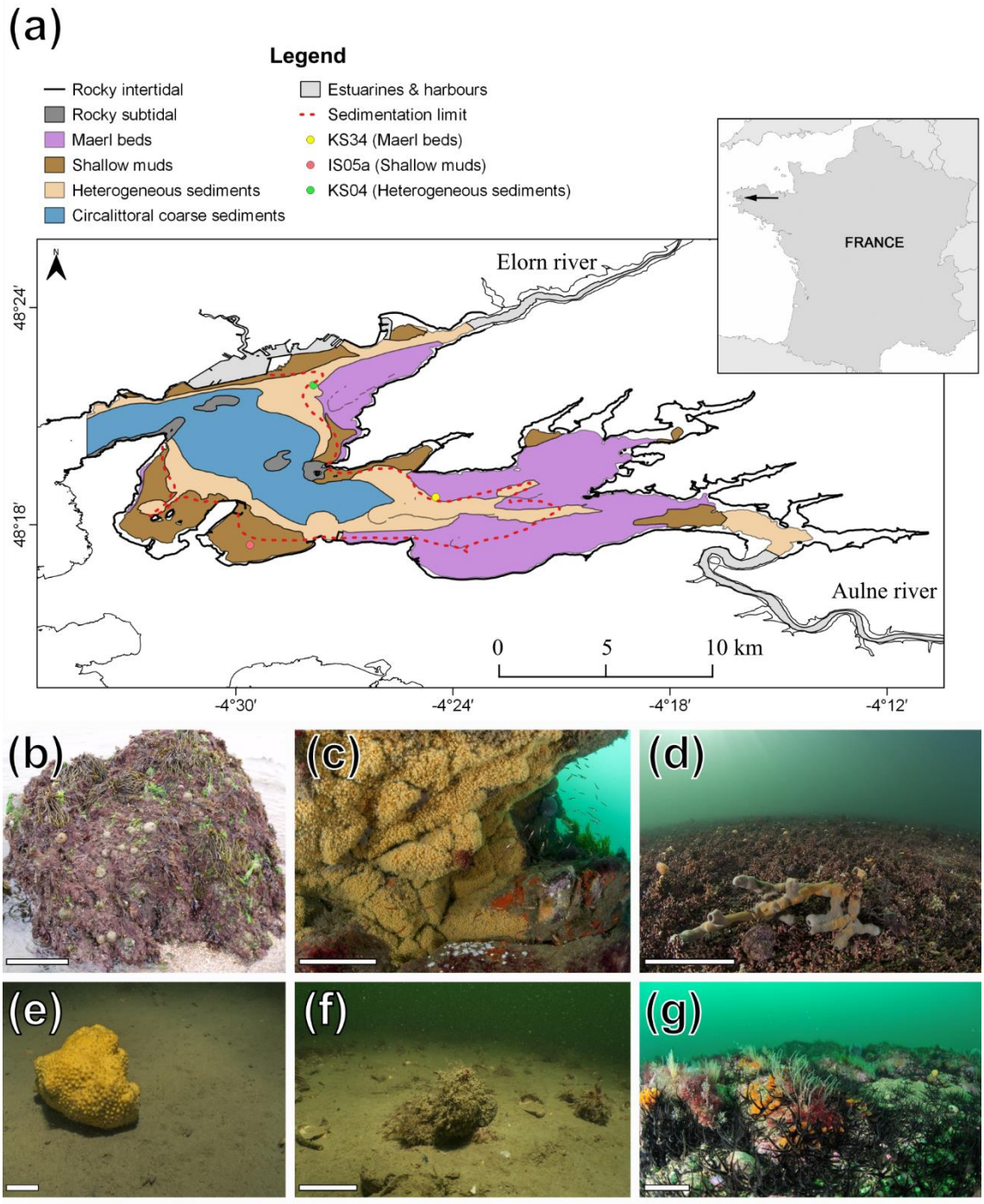

Fig. 1. (a) Map of the Bay of Brest (France), showing the six major habitats defined for this study according to their depth, substrate type, and sponge fauna. Estuaries and harbors, depicted in grey in the map, have not been considered in the study. Red dashed line indicates the limit of sedimentation in the Bay, under which the sedimentation rate is negligible. Circles indicate the geographical

location of the examined cores. (**b-g**) General view of the habitats of the Bay: (**b**) rocky intertidal, (**c**) rocky subtidal, (**d**) maerl beds, (**e**) shallow muds, (**f**) heterogeneous sediments, and (**g**) circalittoral coarse sediments. Scale bars indicate 10 cm.

The Bay hosts abundant and diverse benthic communities, developed in a mixture of hard and soft substrates (Grall and Glémarec 1997). The benthic ecosystem of the Bay consist of six major habitats, according to depth, nature of substrate, and biota (Hily et al. 1992; Gregoire et al. 2016): 1) the rocky intertidal coastline that remains emerged during spring low tides; 2) the rocky subtidal bottoms, down to 20 m depth, that mostly surround the islets of the Bay; 3) the maerl beds, soft bottoms with dense assemblages of *Lithophyllum* spp. down to 15 m depth; 4) the shallow mud bottoms down to 10 m depth, mostly in the peripheral zones of the Bay; 5) the heterogeneous sediments from 5 to 25 m depth which consist of a mix of mud, calcareous detritus, and gravel bottoms; and 6) the circalittoral coarse sediments, consisting of gravel and pebble bottoms located mostly in the central, deepest zones (20 to 40 m) of the Bay (Fig. 1a-g). Using QGIS software, version 3.10.2 (QGIS Development Team 2020), the benthic habitats of the Bay were delimited and their areas were calculated (Fig. 1a; Table 1). This resulted in the most updated map of the benthic habitats of the Bay of Brest, which includes the up-to-date information of the bottom communities of the Bay from the annual monitoring conducted by the Marine Observatory of the European Institute for Marine Studies (Derrien-Courtel et al. 2019).

Table 1. Features of the benthic habitats of the Bay of Brest (France), including bottom area (10^6 m^2), relative contribution (%), sampled area (m^2), mean (±SD) depth (m), and richness of

siliceous species of each habitat and the total Bay. RI, rocky intertidal; RS, rocky subtidal; MB, maerl beds; SM, shallow muds; HS, heterogeneous sediments; CS, circalittoral coarse sediments.

Habitat	Bottom area (10^6 m^2)	Sampled area (m^2)	Depth (m)	Si species richness
RI	1.98 (1.5%)	23	0.0 (± 0.0)	4
RS	2.64 (2.0%)	31	12.4 (± 4.0)	31
MB	45.84 (34.4%)	40	5.4 (±1.6)	19
SM	22.19 (16.7%)	17	5.1 (± 3.0)	2
HS	31.79 (23.9%)	36	11.4 (± 3.7)	16
CS	28.69 (21.6%)	23	25.6 (± 4.5)	32
Total	133.13 (100%)	170	9.9 (± 8.1)	45

Silicon standing stock in sponge communities

To estimate the Si standing stock of the sponge communities within the Bay of Brest, quantitative surveys were conducted across the six benthic habitats. The sampling effort carried out within a given habitat depended on both its relative surface to the total Bay extension and the relative internal variation (Eberhardt 1978). Three sampling techniques were used for the different habitats: (1) the rocky intertidal was sampled by using 23 random quadrats (1×1 m) at low tides; (2) the rocky subtidal, the maerl beds, the shallow mud, and the heterogeneous sediments above 20 m depth were sampled by scuba diving using 119 random 1×1 m quadrats; (3) the heterogeneous sediment and circalittoral coarse sediment located below 20 m depth were sampled using an epibenthic trawl over small transects (1 m wide × 5–10 m long, trawl length precision = ± 1m; n= 28). Each sponge found within the quadrats or in the trawls was counted, taxonomically identified to the species level, and measured for volume and silica content (i.e., biogenic silica, bSi). To determine the sponge volume, the body shape of each individual was approximated to one or a sum of several geometric figures (e.g., sphere, cylinder, cone, rectangular plate, etc.) and the linear parameters needed to calculate the volume (length, width, and/or diameter) were measured in situ using rulers (Maldonado et al. 2010).

Counts and volume values in each habitat were normalized to m^2. Non-siliceous sponge species were taxonomically identified but not considered in the calculations.

The relationship between the mean siliceous sponge abundance (i.e., number of individuals) and biomass (i.e., volume) in each habitat was normalized per m^2 and analyzed by Spearman rank correlation. Between-habitat differences in the sponge abundance and biomass per m^2 were examined by Kruskal-Wallis analysis when data did not meet normality and/or equal variance, following Shapiro-Wilk and Brown-Forsythe tests, respectively. Post-hoc pairwise multiple comparisons between groups were conducted using the non-parametric Dunn's test.

To estimate sponge silica content in a given sponge volume, a plastic cylinder of known volume was filled with sponge tissue (n = 3 to 5 for each species, depending on availability), applying minimum compression. Sponge tissue samples were then dried at 60ºC to constant dry weight (g), and desilicified by immersion in 5% hydrofluoric acid solution for 5 hours, rinsed in distilled water three times for 5 minutes, and dried again at 60ºC to constant dry weight (Maldonado et al. 2010). Silica content per unit of sponge volume (mg bSi mL^{-1} sponge) was calculated as the difference in weight before and after desilicification and multiplied by a factor of 0.8. Such a factor was applied to remove overestimates of the skeletal biogenic silica due to tiny sand grains (lithogenic silica) that might be embedded into the sponge tissues (Maldonado et al. 2010).

Mean skeletal content (mg bSi mL^{-1} sponge) of each species was subsequently used to estimate Si standing stock in the sponge communities per unit of bottom area in the six habitats of the Bay, and that at the ecosystem level. Between-habitat differences in mean sponge Si standing stock per m^2 were examined by a Kruskal-Wallis analysis, followed by pairwise Dunn's tests to identify significant differences between groups. Finally, the relationship between skeletal content and sponge abundance per m^2 and that between skeletal content and sponge biomass per m^2 in the sponge communities of the Bay were also examined using regression analysis.

Dissolved silicon consumption by sponge communities

The annual consumption of dSi (and consequently biogenic silica production) by the sponge communities of the Bay was estimated by using the dSi consumption kinetic models developed elsewhere (López-Acosta et al. 2016, 2018) for the four dominant sponge species at the Bay (*Haliclona simulans*, *Hymeniacidon perlevis*, *Tethya citrina*, and *Suberites ficus*). By knowing the monthly average dSi availability in the bottom waters of the Bay over the last decade (2012-2021; Table S1) and the consumption kinetics of each of the four dominant species at the Bay, the average (±SD) annual dSi consumption rate by these species was estimated. This average was then extrapolated to the rest of the sponge species in the Bay to estimate dSi consumption by habitat and for the entire Bay, according to the previously estimated species sponge biomass per habitat (mL sponge m^{-2}) and habitat bottom area (m^2).

Sponge biogenic silica in superficial sediments

The amount of sponge Si in the sediments was determined by analyzing superficial sediments samples (defined herein as the upper-centimeter layer of sediment) from three stations from the shallow plateaus of the Bay of Brest (Fig. 1a). In the Bay, there are two major depositional environments with contrasting features: 1) the shallow terraces or plateaus, up to 10 m depth, where the fine sediment that regularly arrives through the rivers' discharges is homogeneously deposited, and 2) the deepest bottoms, up to 40 m depth, where the strong tidal currents prevent the fine sediment from being deposited on the bottom (Salomon and Breton 1991; Gregoire et al. 2017; Lambert et al. 2017). The latter are located mainly in the central zone of the Bay and the two paleo-channels that cross each of the basins of the Bay from the rivers' mouths to the central zone, where

they converge (see Figure 1 in Gregoire et al. 2017). This depositional configuration was originated by the action of successive sea-level low stands and it has been preserved over the last millennia by the effect of tidal currents in deep-water areas, which keep the inherited shape by preventing the deposition of the fine sediment supplied by rivers (Gregoire et al. 2016, 2017). As a consequence of this hydrodynamic regime, the fine sediment does not settle on the deepest areas of the Bay, the sediments of which mainly consist of coarse particles such as gross fragments of shells and small pebbles (Gregoire et al. 2016). On the contrary, the fine sediment settles all over the shallow plateaus, which are less affected by the tidal currents. Hence, the shallow plateaus account for virtually the total area of sediment deposition in the Bay bottoms (Ehrhold et al. 2016). These shallow plateaus, which account for about half of the Bay surface, are mainly covered by maerl beds, shallow muds and partially by heterogeneous sediments (Fig. 1a; Table 2).

To estimate the amount of sponge silica in the superficial sediments of the Bay, one core was sampled at each benthic habitat represented at the shallow plateaus: core SRQ3-KS34 from maerl beds, core SRQ1-IS05 from shallow muds, and core SRQ3-KS04 from heterogeneous sediments (Fig. 1a, Table 2). Present-day sedimentation rates were estimated from radiocarbon dating of superficial sediment in the cores (Gregoire et al. 2017; Ehrhold et al. 2021). The bottoms of the deepest areas of the Bay, on which sedimentation rates are negligible (Ehrhold et al. 2016), were interpreted as null contributors to the sponge silica accumulation in the Bay (see below).

Table 2. Summary of core features including core label, coordinates, depth (m), average (±SD) sedimentation rate (cm y^{-1}), the benthic habitat compartment they represent, and the extension of the benthic habitat over the sedimentation limit of the Bay (km^2). Present-day sedimentation

205 rates for the superficial sediments of each core were estimated from ^{14}C radiocarbon dating in
206 Gregoire et al. (2017) and Ehrhold et al. (2021).

Core label	Coordinates		Depth (m)	Sedimentation rate (cm y^{-1})	Benthic habitat compartment	Compartment extension (km^{-2})
	Latitude	Longitude				
SRQ3-KS34	48º 18.760' N	4º 24.474' W	10	0.037 (± 0.003)	Maerl beds (MB)	40.06
SRQ1-IS05a	48° 17.441' N	4° 29.609' W	7	0.090 (± 0.002)	Shallow muds (SM)	17.21
SRQ3-KS04	48° 21.858' N	4° 27.857' W	7	0.077 (± 0.001)	Heterogeneous sediments (HS)	9.18

207

208

209 To quantify the sponge silica in the superficial sediment layer, one to three sediment subsamples
210 of 10 mg each were collected from the upper 1-cm layer of each core and subsequently processed by
211 light microscopy, following the methodology described in Maldonado et al. (2019). Briefly, sediment
212 subsamples were transferred to test tubes, boiled in 37% hydrochloric acid to remove calcareous
213 materials, then in 69% nitric acid to complete digestion of organic matter, rinsed in distilled water,
214 and sonicated for 15 minutes to minimize sediment aggregates. The sediment suspension was then
215 pipetted out and dropped on a microscope glass slide to measure the volume of each skeletal piece. A
216 total of 230 smear slides in which 48320 spicules, either entire or fragmented, were examined
217 through contrast-phase compound microscopes. Using digital cameras and morphometric software
218 (ToupView, ToupTek Photonics), the volume of each spicule or spicule's fragment was estimated by
219 approximating its shape to one or the sum of several geometric figures (Maldonado et al. 2019).
220 Measured volumes of sponge silica were subsequently converted into Si mass, using the average
221 density of 2.12 g mL^{-1} for sponge silica (Sandford 2003).

222 To determine the reservoir of sponge silica in the superficial sediment of the Bay, the obtained
223 mass of sponge silica per gram of sediment in each core was extrapolated to the area of each benthic
224 habitat over the sedimentation limit, delimited with a red dashed line in Figure 1 from the

sedimentological data published in Ehrhold et al. (2016). It means that the sponge silica mass per gram of sediment from core SRQ3-KS34 was extrapolated to 40.06 km^2, that of core SRQ1-IS05 to 17.21 km^2, and that of core SRQ3-KS04 to 9.18 km^2 (Table 2). Sponge Si deposition rate was estimated from the amount of sponge Si determined in the superficial sediments of each core and the sedimentation rate (Table 2). Sponge Si burial rate, i.e., the amount of sponge silica that is ultimately preserved in the sediments, was estimated from the rate of sponge Si deposited annually in the superficial sediments and the average percentage estimated for sponge Si preservation in sediments of marine continental shelves (i.e., 52.7 ± 29.8%; Maldonado et al., 2019). The contribution of sponges to the Si benthic efflux from the sediments of the Bay was calculated as the difference between the sponge Si deposition and burial rates.

Sponge silica budget in a coastal ecosystem: the Bay of Brest

The quantified stocks and fluxes of sponge Si were used to build a sponge Si budget for the Bay of Brest. These results were discussed in the context of previous studies and compared with those reported in the literature for the community of planktonic diatoms in the Bay.

Results

General features of the sponge assemblages

The survey of the sponge fauna at the Bay of Brest revealed a total of 53 sponge species, most of them belonging to the class Demospongiae (n=51), and only 2 species belonging to the class Calcarea (Table S2). Species from classes Hexactinellida and Homoscleromorpha were not found. Forty-five (85%) of the 53 identified species had siliceous skeletons. The other 8 were non-siliceous sponge

247 species with a skeleton made of either calcium carbonate (n=2) or skeletal protein (n=6). Non-
248 siliceous sponges were not considered in the following quantifications of sponge abundance and
249 biomass.

250 Sampling yielded a total of 1807 sponge individuals for which volume was determined (Table 1).
251 At the Bay level, the siliceous sponge fauna averaged 11.0 ± 11.1 individuals m^{-2} and a biomass of
252 0.31 ± 0.35 L of living sponge tissue m^{-2}. The large variation associated (i.e., standard deviation, SD)
253 to the sponge abundance and biomass normalized per m^2 is derived from the patchy spatial
254 distribution of the sponges at both intra- and inter-habitat level. In contrast, the standard error (SE) of
255 the mean (=SD/√N) is low (SE of sponge abundance = 0.85; SE of sponge biomass = 0.03),
256 indicating that mean values are accurate. A Spearman's correlation involving the six habitats
257 revealed a strong positive linear relationship between the mean abundance and biomass of siliceous
258 sponges per m^2 of sampled bottom (N = 6, ρ = 0.886, p = 0.033). This relationship informs that body
259 size is more or less uniformly distributed across species and specimens of the different habitats.

260 At the habitat level, there were large between-habitat differences in both sponge abundance and
261 biomass (Fig. 2). The total number of siliceous sponges per m^2 significantly differs between habitats
262 (H= 89.059, df= 5, p< 0.001). Mean siliceous sponge abundance per m^2 in the benthic communities
263 of the maerl beds and rocky subtidal habitats (24.6 ± 26.2 and 16.4 ± 9.3 individuals m^{-2},
264 respectively) were significantly higher than that in the other habitats (Fig. 2a). Biomass of siliceous
265 sponges (L m^{-2}) also differed significantly between habitats (H= 78.324, df= 5, p< 0.001). A
266 posteriori pairwise comparison revealed that mean sponge biomass per m^2 at the rocky subtidal
267 habitat, which showed the highest sponge biomass per sampled bottom (3.8 ± 9.7 L m^{-2}), was
268 significantly higher than that at the heterogeneous sediments (0.16 ± 0.38 L m^{-2}) and the rocky
269 intertidal (0.12 ± 0.13 L m^{-2}) habitats. Mean sponge biomass per m^2 at maerl beds (0.31 ± 0.32 L m^{-2}), which ranked second, did not differ significantly from that at the rocky subtidal, either at the

271 heterogeneous sediments and rocky intertidal habitat. Mean sponge biomass per m^2 at shallow muds
272 and circalittoral coarse sediments were similar to each other and significantly lower than those at the
273 rest of habitats in the Bay (Fig. 2b-c).

274

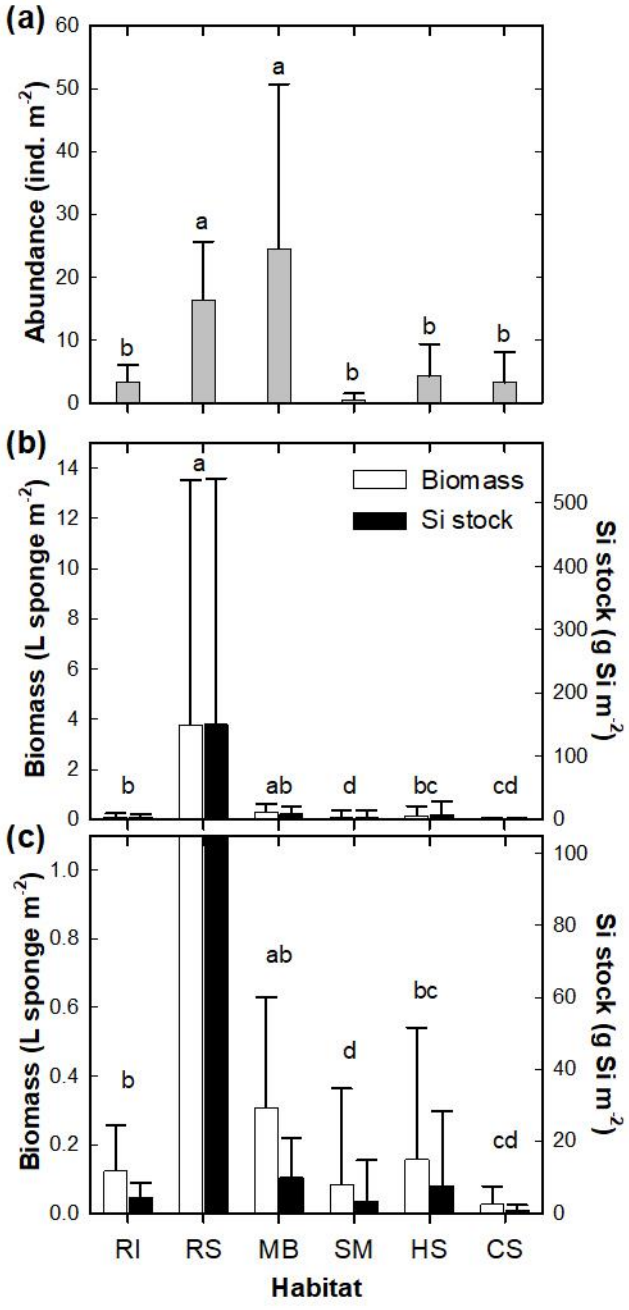

275

Fig. 2. Summary of (a) average (±SD) abundance (individuals m^{-2}), (b-c) biomass (L sponge m^{-2}; white bars), and silicon (Si) standing stock (g Si m^{-2}; black bars) in the siliceous sponge fauna of the habitats of the Bay of Brest (France). Significant between-habitat differences of (**a**) abundance and (**b**) biomass and Si stock of the sponge fauna are indicated with different letters according to the results of Kruskal-Wallis analysis and the a posteriori pairwise Dunn's tests. (**c**) This graph makes visible the contribution of the habitats with sponge biomass and Si standing stock records lower than 1 L sponge m^{-2} and 100 g Si m^{-2}. Habitats abbreviations are RI for rocky intertidal, RS for rocky subtidal, MB for maerl beds, SM for shallow muds, HS for heterogeneous sediments, and CS for circalittoral coarse sediments.

Silicon standing stock in the sponge communities

The importance of the siliceous skeleton content per mass unit of sponge tissue varied largely between sponge species (Table 3). It ranged from 29.8 ± 2.9 to 145.6 ± 14.2 mg bSi per mL of living sponge tissue (Table 3), accounting for 19.6% to 63.5% of the specific dry weight (DW). The average skeletal content estimated for the siliceous sponge fauna of the Bay of Brest was 59.6 ± 27.1 mg bSi mL^{-1} (45.8 ± 10.6% bSi/DW). From these figures, it is estimated that the Si standing stock in the sponge fauna of the Bay of Brest is 12.3 ± 14.1 g Si m^{-2}. Nevertheless, there are large between-habitat differences in the sponge Si standing stock per m^2 (Fig. 2b-c). The highest mean Si standing stock occurred in the rocky subtidal habitat (151.1 ± 387.6 g Si m^{-2}). At this habitat, large specimens of *Cliona celata* were common (mean abundance= 0.5 ± 0.7 individual m^{-2}, mean biomass= 7.4 ± 13.5 L $individual^{-1}$). The large specimens of this species, which is moderately silicified (85.6 ± 7.2 mg bSi mL^{-1}; Table 3), are responsible for the 89.2% of the total biomass and Si standing stock of the rocky subtidal habitat. The maerl beds ranked second in Si standing stock, with an average of 10.0 ±

299 10.7 g Si m^{-2} (Fig. 2b-c). In this habitat there is large abundance of sponges (24.6 ± 26.2 individuals
300 m^{-2}) with body size ranging from small to medium (mean biomass= 12.4 ± 37.1 mL $individual^{-1}$).
301 Four of the 19 siliceous sponge species identified at this habitat accounted for 84% of the total
302 sponge Si standing stock (*Haliclona simulans*, *Hymeniacidon perlevis*, *Tethya citrina*, and *Suberites*
303 *ficus*). A Kruskal-Wallis analysis confirmed that the between-habitat differences in sponge Si
304 standing stock per m^2 are statistically significant (H = 71.701, df = 5, p<0.001). The pairwise
305 comparison of mean Si standing stock revealed the same pattern of between-habitat differences than
306 that obtained in the pairwise comparison of mean sponge biomass (Fig. 2b-c). Further analysis
307 indicated a significant linear relationship (n= 170, R^2= 0.999, p<0.0001) between sponge biomass
308 and Si standing stock per m^2 across habitats (Fig. 3).

309

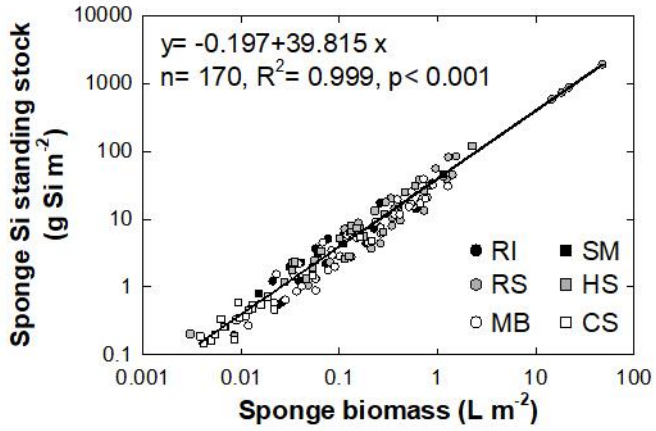

310

311 **Fig. 3. Relationship between silicon (Si) standing stock (g Si m^{-2}) and biomass (L m^{-2}) of**
312 **siliceous sponges per m^2 of sampled bottom at the Bay of Brest (France).** Symbols represent the
313 location of the data (i.e., habitat; abbreviations mean: RI, rocky intertidal; RS, rocky subtidal; MB,
314 maerl beds; SM, shallow muds; HS, heterogeneous sediments; CS, circalittoral coarse sediments).
315 Sponge Si stock and biomass are shown in logarithmic scale.

316

317 By integrating the average Si content of the sponges across the bottom area of each habitat, a total
318 Si standing stock of 1215 ± 1876 x 10^3 kg Si (43.3 ± 66.8 x 10^6 mol Si) in the sponge communities of
319 the Bay of Brest was estimated. The small-scale patchiness in the spatial distribution of the sponges
320 within a habitat causes some sampling quadrats to contain many sponges while others contain very
321 few or none. This effect, when propagated for the calculation of the global mean of the Bay, results in
322 a large SD value. In addition, about 90% of the stock is accumulated in the sponge fauna of three
323 habitats, which —in order of contribution— are the maerl beds, the rocky subtidal, and the
324 heterogeneous sediments.

325

326 **Dissolved silicon consumption by sponge communities**

327 The average monthly concentrations of dSi at the bottom waters of the Bay ranged from 2 to 13
328 µM (Table S1). At these nutrient concentrations, the most abundant species at the Bay (*H. perlevis*,
329 68.6 ± 85.1 mL m^{-2}) consumed 7.2 ± 8.9 mmol Si m^{-2} y^{-1}. Interestingly, the species *T. citrina* and *S.*
330 *ficus*, which show comparatively lower biomass records in the Bay (24.5 ± 34.1 and 7.7 ± 13.3 mL
331 m^{-2}, respectively), had similar rates of Si consumption (7.5 ± 10.5 and 7.1 ± 21.0 mmol Si m^{-2} y^{-1},
332 respectively). This is because their affinity for dSi is higher (affinity coefficient, V_{max}/K_M = 6.9 x 10^{-3}
333 and 4.4 x 10^{-3} µmol Si h^{-1} sponge-mL^{-1} Si-μM^{-1} for *T. citrina* and *S. ficus*, respectively, compared to
334 2.1 x 10^{-3} µmol Si h^{-1} sponge-mL^{-1} Si-μM^{-1} for *H. perlevis*).

335 Not surprisingly, most of the sponge Si consumption of the Bay occur in the rocky subtidal habitat
336 and maerl beds, where sponges are very abundant and they show moderate to large biomass records
337 (Fig. 2). The rocky subtidal habitat, which represents only 2.0% of the Bay bottom but hosts about
338 30% of the total sponge biomass in the Bay, shows an annual sponge Si consumption rate of 74.2 ±

141.4 x 10^3 kg Si y^{-1} (2.6 ± 5.0 x 10^6 mol Si y^{-1}). The maerl beds, in which *H. perlevis*, *T. citrina*, and *S. ficus* are abundant in both terms of number of individuals and biomass, shows an annual Si consumption rate of 73.6 ± 112.7 x 10^3 kg Si y^{-1} (2.6 ± 4.0 x 10^6 mol Si y^{-1}). Collectively, the assemblage of siliceous sponges in the Bay is estimated to consume annually 200.8 ± 372.1 x 10^3 kg Si y^{-1} (7.2 ± 13.2 x 10^6 mol Si y^{-1}).

Sponge bSi in sediments

The superficial sediments (i.e., the upper 1-cm layer) of cores SRQ3-KS34, SRQ1-IS05a, and SRQ3-KS04, contained respectively a total of 1.07 (±0.05), 1.30, and 0.32 million spicules or spicule fragments per g of sediment, with an average spicule content of 0.89 (±0.51) million spicules g^{-1} sediment for the set of studied cores (Table 4). In all cores, most spicules (98.3-99.1%) were recognized as megascleres, either entire or fragmented. The microscopic study of the superficial sediment in the cores showed only small between-area differences in the mass of sponge bSi, which ranged from 0.799 to 2.505 mg Si g^{-1} sediment (Table 4). The average content of sponge bSi in the sediments of the Bay of Brest was 1.565 (±0.866) mg Si g^{-1} sediment.

Table 4. Summary of the results obtained during the microscopic examination of the superficial sediments of the Bay of Brest. Average (±SD, when available) spicule counts (in millions per gram of sediment), contribution (%) of megascleres (spicules longer than 100 µm) and microscleres (spicules shorter than 100 µm), and mass of sponge silica per gram of sediment for each core are indicated, as well as for the set of study cores.

Core label	Benthic habitat	N spicules (N x 10^6 g^{-1} sed.)	Spicule-type contribution (%)		Sponge Si in superficial sed. (mg Si g^{-1} sed.)
			Megascleres	Microscleres	
SRQ3-KS34	Maerl beds (MB)	1.07 (± 0.05)	99.1 (± 0.3)	0.9 (± 0.3)	1.391 (± 0.241)
SRQ1-IS05a	Shallow muds (SM)	1.30	99.0	1.0	2.505
SRQ3-KS04	Heterogeneous sediments (HS)	0.32	98.3	1.7	0.799
AVERAGE (±SD)		0.89 (± 0.51)	98.8 (± 0.4)	1.2 (± 0.4)	1.565 (± 0.866)

Sponge Si deposition rates in the studied areas ranged from 9.4 to 64.4 x 10^3 kg Si y^{-1}, depending on the habitat (Table 5). When deposition rates were extrapolated to the total extension of the shallow plateaus (i.e., 66.45 km^2), it resulted in a mean deposition rate of 108.7 ± 9.1 x 10^3 kg Si y^{-1} (3.9 ± 0.3 x 10^6 mol Si y^{-1}). The sponge Si burial rate was then calculated from the deposition rate and the average preservation rate of sponge silica determined by Maldonado et al. (2019) for continental-shelf sediments. This approach yielded an average burial rate of sponge silica in the sediments of the shallow plateaus of 57.3 ± 18.2 x 10^3 kg Si y^{-1} (2.0 ± 0.6 x 10^6 mol Si y^{-1}). The differences between deposition and burial rate is, in the long run, the sponge contribution to the benthic Si efflux from sediments, which was estimated to be 51.4 ± 17.7 x 10^3 kg Si y^{-1} (1.8 ± 0.6 x 10^6 mol Si y^{-1}) for the shallow plateaus of the Bay (Table 5).

Table 5. Sponge silicon (Si) stock in the superficial sediments of each depositional environment of the Bay of Brest, along with the deposition, burial and benthic flux rate of sponge Si. Area (km^2) to which the sponge Si data were extrapolated is indicated. These areas do not correspond to the total habitat extension but to the habitat area that is above the sedimentation limit of the Bay (indicated with a red dashed line in Fig. 1a) for cores representing the shallow depositional plateaus.

Core label	Benthic habitat	Area	Sponge Si STOCK	Sponge Si FLUXES		
			reservoir	deposition rate	burial rate	benthic flux
		km^2	10^3 kg Si	10^3 kg Si y^{-1}	10^3 kg Si y^{-1}	10^3 kg Si y^{-1}
SRQ3-KS34	Maerl beds (MB)	40.06	937.93	34.91	18.39	16.52
SRQ1-IS05a	Shallow muds (SM)	17.21	715.41	64.39	33.92	30.47
SRQ3-KS04	Heterogeneous sediments (HS)	9.18	121.70	9.38	4.94	4.44
TOTAL		66.45	1775.04	108.68	57.25	51.43

According to the depositional environments of the Bay, the deep sediments were not considered in the calculations of the total sponge Si reservoir and sediment fluxes rates (see Methods). This is also supported by the sponge spatial distribution at the Bay, which shows that in the deepest areas sponges are particularly low abundant (3.2 ± 4.9 ind. m^{-2}) and their contribution to the Si standing stock is significantly low (0.8 ± 1.4 g Si m^{-2}; Fig. 2). By extrapolating the sponge silica content determined in the superficial sediments of the Bay (Table 5), a total sponge silica reservoir in the superficial (upper centimeter) sediment layer of the Bay of Brest of 1775 ± 162 x 10^3 kg Si (63.2 ± 5.8 x 10^6 mol Si) was estimated.

Discussion

Sponge fauna within the Bay of Brest

The survey of the sponge fauna of the Bay of Brest revealed that sponges are ubiquitous and widely present in most of the habitats (17-36 spp. per habitat; Table 1, Fig. 2, Table S2). Only two habitats, the shallow muds and the rocky intertidal, showed low sponge species richness (≤ 4 species per habitat; Table 1, Table S2). These two habitats, the former characterized by muddy bottoms and scanty hard

395 substratum and the latter by periodic air exposures during low tides, hosted only a handful of species
396 able to deal with those harsh conditions (Table S2).

397 The taxonomic composition and spatial distribution of the sponge fauna significantly differed
398 between habitats (Table 1, Fig. 2). Spatial heterogeneity has been widely reported for sponge
399 distributions across all oceans, with a variety of biological and physical reasons behind it (Hooper
400 2019). Among the habitats of the Bay, the rocky subtidal is the one with the highest sponge biomass
401 per unit area (3.8 ± 9.7 L m^{-2}; Fig. 2b), reaching values similar to those reported in some emblematic
402 sponge aggregations in tropical and polar latitudes (Maldonado et al. 2017 and references therein).
403 According to their extension, the maerl beds, which accounted for about one third of the total surface
404 of the Bay (Table 1), hosted most of the sponge individuals and biomass of the Bay —79 ± 46% of the
405 total number of sponges (1416 ± 1474 million of individuals) and about 44 ± 23% of the total sponge
406 volume (31.9 ± 47.0 x 10^6 L) estimated at the Bay of Brest. Thus, the maerl beds of the Bay serve as
407 substrate to highly diverse and abundant sponge fauna, which along with other benthic organisms,
408 make these bottoms real sponge and biodiversity hotspots, similar to what has been reported for maerl
409 beds from other ocean regions (Sciberras et al. 2009; Ávila and Riosmena-Rodriguez 2011; Neill et al.
410 2015).

411

412 **Biogenic silica stock as sponge skeletons**

413 Our results indicate that a substantial amount of the biogenic silica stock of the Bay of Brest is in
414 the form of sponge silica, in both the living sponge fauna and the sediments of the Bay (Fig. 4). In
415 the sponge communities, the Si standing stock within the skeleton of the sponges totaled 1215 ± 1876
416 x 10^3 kg of Si. The siliceous skeleton accounted for 19.6-63.5% of the sponge dry weight, depending
417 on the species (average value = 45.8 ± 10.6% bSi/DW = 59.6 ± 27.1 mg bSi mL^{-1}; Table 3). Similar

418 bSi content and between-species variability was also reported in a sponge-rich community of the
419 Belizean Mesoamerican Barrier Reef (53.4 ± 6.1 mg bSi mL^{-1}; Maldonado et al. 2010).

420 To date, only few studies have measured the amount of Si trapped in sponge communities of
421 shallow-water ecosystems. The sponge Si standing stock per m^2 in the Bay of Brest (12.3 ± 14.1 g Si
422 m^{-2}) is about 5 times higher than that found in the sublittoral population of the encrusting
423 demosponge *Crambe crambe* at the Catalan coast of the NW Mediterranean (2.5 ± 2.7 g Si m^{-2};
424 Maldonado et al. 2005) and, interestingly, similar to that measured in the sublittoral sponge-rich
425 assemblages of the Belize section of the Mesoamerican Barrier Reef (12.0 g Si m^{-2}; Maldonado et al.
426 2010). The sponge Si standing stock of the Bay of Brest is also similar to that found at bathyal depths
427 at the westward slope of the Mauna Loa Volcano of Hawaii (12.6 g Si m^{-2}; Maldonado et al. 2005),
428 where a dense monospecific population of the highly-silicified hexactinellid *Sericolophus hawaiicus*
429 occurs. Higher records of Si sponge stocks have only been reported from 1) the monospecific sponge
430 ground of the hexactinellid *Vazella pourtalessii* at the Nova Scotian continental shelf, Canada (43.8 ±
431 74.6 g Si m^{-2}; Maldonado et al. 2021), 2) the continental margins of Antarctica (178 g Si m^{-2}; Gutt et
432 al. 2013), where heavily silicified demosponges and hexactinellids co-occur, and 3) the singular
433 epibathyal reefs of the hexactinellid *Aphrocallistes vastus* in British Columbia (Canada), where high
434 densities of heavily silicified individuals grow on exposed skeletons of dead sponges, leading to
435 outstanding accumulations of sponge silica in the form of siliceous reefs (4238 ± 924 g Si m^{-2}; Chu et
436 al. 2011). Altogether, these results support the idea that sponge communities are transient Si sinks
437 (Maldonado et al. 2005, 2010) and suggest that relevant standing stocks of sponge silica are likely to
438 occur not only in deep-sea and polar latitudes but also in shallow-water ecosystems from temperate
439 latitudes, in which diverse and abundant sponge populations may easily develop (Van Soest et al.
440 2012; Maldonado et al. 2017).

441 The amount of sponge silica accumulated in only the superficial (upper centimeter) sediment layer
442 of the Bay of Brest (1775 ± 162 x 10^3 kg Si; Fig. 4) falls in the same order of magnitude than that
443 accumulated in the living sponge fauna of the Bay (1215 ± 1876 x 10^3 kg; Fig. 4). The Si stock in the
444 superficial sediments is in the form of siliceous spicules that reach the sediments after sponge death
445 (Chou et al. 2012; Lukowiak et al. 2013; Maldonado et al. 2019), the abundance of which appears to
446 be proportional to the silica standing stock in the sponge communities living nearby (Bavestrello et
447 al. 1996; Lukowiak et al. 2013). The amounts of sponge silica deposited on the superficial sediments
448 of the Bay of Brest (0.799 – 2.505 mg Si g^{-1} sediment; Table 4) are among the highest determined in
449 superficial sediments of continental margins from different oceans and seas (0.014 – 2.572 mg Si g^{-1}
450 sediment; Sañé et al. 2013; Maldonado et al. 2019). For instance, the amount of sponge silica
451 determined in the superficial sediments of the shallow muds (2.505 mg Si g^{-1} sediment, core SRQ1-
452 IS05a; Table 4) is nearly identical to that determined in the superficial sediments of the slope of the
453 Bransfield Strait in Antarctica (2.572 ± 0.861 mg Si g^{-1} sediment; Maldonado et al. 2019), where
454 dense sponge aggregations occur (Ríos and Cristobo 2014; Kersken et al. 2016; Gutt et al. 2019).
455 Combining the cores examined in this study (1.565 ± 0.241 mg Si g^{-1} sediment), the sediments of the
456 Bay had about 60% more sponge silica than the average estimated for the sediments of continental
457 margins in the global ocean (0.924 ± 0.854 mg Si g^{-1} sediment; Maldonado et al., 2019), indicating
458 that sediments from areas where sponges abound become an important reservoir of biogenic silica.

459

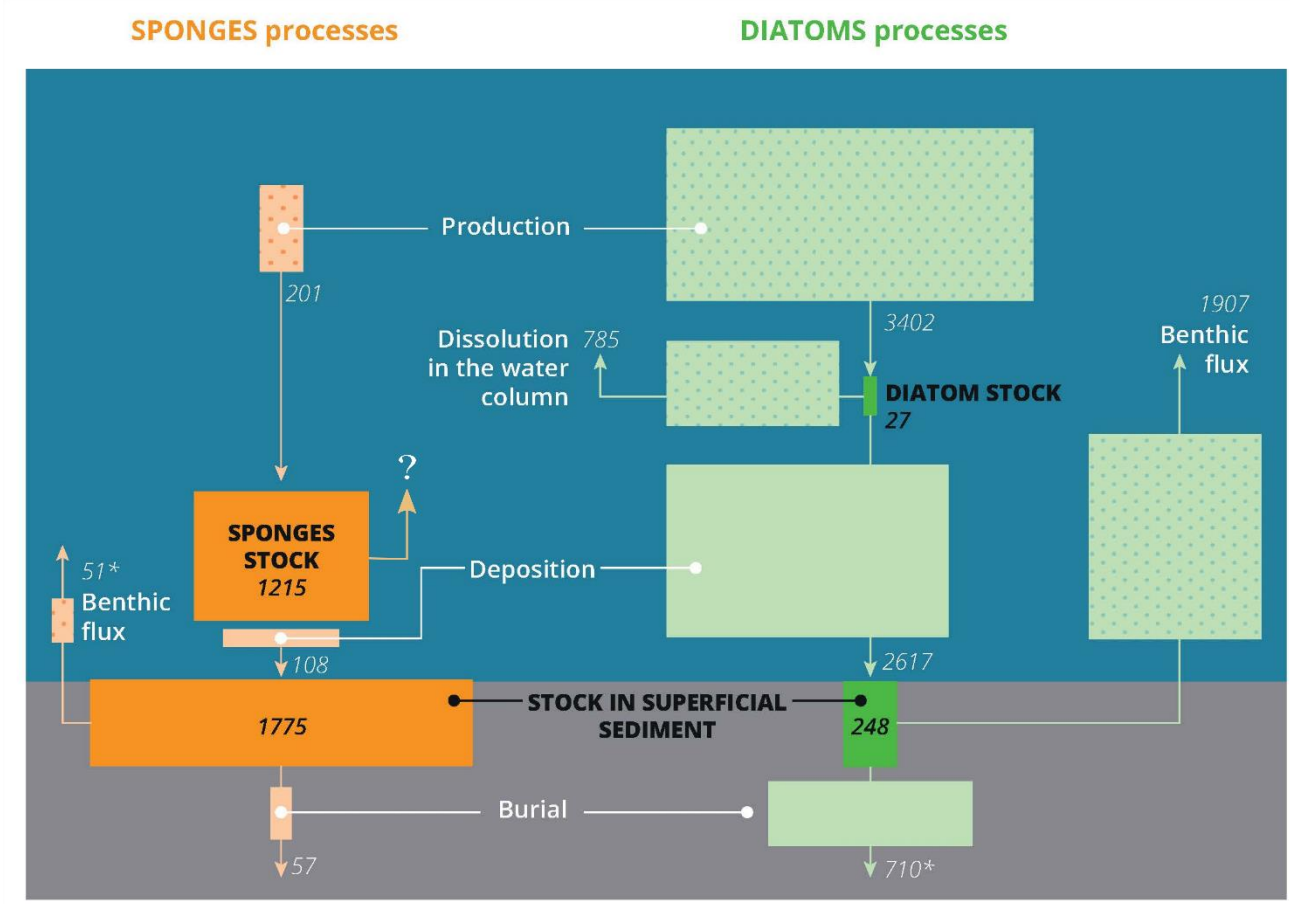

460

461 **Fig. 4. Scheme summarizing the silicon stocks and fluxes through the sponge and planktonic**
462 **diatom communities of the Bay of Brest (France).** Stocks and fluxes of silicon (Si) mediated by
463 sponges are in orange, and those mediated by diatoms are in green. Stocks of biogenic silica are
464 indicated in tons of Si. Fluxes of silicic acid, with a dotted pattern, and those of biogenic silica,
465 lacking the dotted pattern, are indicated in tons of Si per year. The size of the boxes representing both
466 stocks and fluxes is proportional to their rate. Fluxes of Si through diatoms are from Ragueneau et al.
467 (2005), stock of biogenic silica in planktonic diatoms has been calculated from Beucher et al. (2004),
468 and reservoir of diatom silica in superficial sediments are from Song and Ragueneau (2007); more
469 details about calculations in the main text. Asterisks (*) refer to fluxes derived indirectly.

470

Silicon cycling through the sponge assemblage

The siliceous skeletons produced by the sponges as part of their annual growth are progressively accumulated within the sponge body for the lifespan, which is thought to range from years to decades or centuries in shallow-water sponge species from temperate latitudes (McMurray et al. 2008; Teixidó et al. 2011; McGrath et al. 2018). When a sponge dies or part of its body is removed or damaged by either natural or anthropogenic processes, the siliceous spicules within the sponge tissue are freed and end deposited on the superficial sediments (Chou et al. 2012; Lukowiak et al. 2013; Maldonado et al. 2019). In the Bay of Brest, the deposition of sponge silica was estimated to be 108 ± 9 x 10^3 kg Si y^{-1} (Fig. 4). Such rate is about twice smaller than the rate at which sponges produce silica in the Bay (201 ± 372 x 10^3 kg Si y^{-1}; Fig. 4). That would mean that the sponge fauna of the Bay of Brest would be increasing at a rate of 92 ± 241 x 10^3 kg Si y^{-1} (3.3 ± 8.6 x 10^6 mol Si y^{-1}), which would double the sponge Si standing stock (i.e., the sponge population) in about 13 years. In contrast, the sponge fauna survey of the Bay over the last 6 years and the long-term survey conducted in the area by the Marine Observatory of the IUEM since 1997 do not indicate that the sponge populations of the Bay are increasing at such high rate, rather the abundance and biomass of the sponge assemblages appear to be relatively constant in the long run (J. Grall, pers. comm.). Other reasons may also contribute to the imbalance between the annual silica production and deposition rates. First, the sponge mortality rate is unlikely to be constant every year. Indeed, a longer time frame (of at least a decade) is likely needed to capture the Si cycling dynamics in the sponge populations (McMurray et al. 2015; Bell et al. 2017). Second, there might be some partial rapid (<1y) dissolution of the spicules upon sponge death. Although sponge silica is more resistant to dissolution than that of others silicifiers (Rützler and Macintyre 1978; Erez et al. 1982; Maldonado et al. 2005, 2019), the most labile fraction of the sponge silica might be dissolved before the spicules being accumulated in the sediments. This would be in agreement with a recent study (Ng et al. 2020) that

has measured through δ^{30} Si that the remineralization of silica from demosponges —the same Class of sponges as those occurring in the Bay of Brest— may be locally significant in superficial sediments where sponges abound. In the study, Ng and co-authors determined that the benthic Si effluxes from bottoms with sponges were from 2 to 10 times higher than those from sediments without sponges. Finally, it cannot be excluded that part of the sponge silica deposited on the Bay bottoms is exported out of the Bay during the monthly strong tidal currents during spring tides or during extreme storms events, the force of which has been suggested to partially transport the deposited sediments of the Bay (Beudin 2014). Further research is necessary to resolve which of these processes, or if a combination of them, could explain the imbalance between the annual sponge silica production and deposition rates at the Bay.

Through deposition, the sponge silica accumulates in the sediments of the Bay and is finally buried at an average rate of 0.06 cm y^{-1} (Gregoire et al. 2017; Ehrhold et al. 2021). Within the first centimeters of marine sediments, biogenic silica —no matter its origin— dissolves progressively until the interstitial water becomes saturated in dSi, an asymptotic condition in which biogenic silica dissolution typically ceases (Rickert et al. 2002; Sarmiento and Gruber 2006; Khalil et al. 2007). In the sediments of the Bay of Brest, the interstitial water reaches dSi asymptote at 10-15 cm burial depth (Raimonet et al. 2013), meaning that below that threshold, the amount of sponge silica buried annually ($57 \pm 18 \times 10^3$ kg Si y^{-1}; Fig. 4) is preserved definitively in the sediments of the Bay. The difference between the sponge silica deposited on superficial sediments and that buried definitively in the sediments ($51 \pm 18 \times 10^3$ kg Si y^{-1}; Fig. 4) is assumed to be dissolved as interstitial dSi during the early steps of burial. Such amount of dSi contributes to the saturation of interstitial water and ultimately feeds the dSi benthic efflux from the sediments of the Bay toward the water column, a recycling process that helps to sustain the populations of planktonic diatoms during the productive season in the Bay (Chauvaud et al. 2000; Ragueneau et al. 2002). Further investigation on the

519 processes involved in the dissolution of sponge silica during the early steps of burial would help to
520 quantify more accurately at which level the sponge Si contributes to the benthic dSi efflux.

521

522 **Sponge vs. diatom Si cycle at the Bay of Brest**

523 The biogeochemical cycling of Si in the Bay of Brest through planktonic diatoms is well studied
524 (e.g., Delmas and Tréguer, 1983; Del Amo et al., 1997; Chauvaud et al., 2000; Beucher et al., 2004)
525 and summarized in Ragueneau et al. (2005). This budget was based on diatom Si flux rates and did
526 not consider the sponge Si flux rates, nor the biogenic silica stocks of sponges and diatoms in the
527 living communities and sediments.

528 To compare the contribution of diatoms and sponges to the Si budget of the Bay, the standing
529 stocks and Si reservoirs in the form of diatom silica were determined from the literature. According
530 to it, the standing stock of diatoms in the water column of the Bay ranges from 0.12 to 1.98 µmol Si
531 L^{-1} over the year cycle (Beucher et al. 2004). Unlike sponges, diatom cells have an ephemeral life of
532 only days. Therefore, the silica standing crop of planktonic diatoms is known to change drastically
533 from week to week and over seasons, depending on nutrient availability and hydrological conditions
534 (Sarthou et al. 2005; Falkowski and Oliver 2007; Armbrust 2009). If the annual mean of diatom silica
535 in the Bay (0.9 µmol Si L^{-1}; Beucher et al. 2004) is homogeneously extrapolated to the whole volume
536 of the Bay of Brest (1.07 x 10^{12} L), an average diatom silica standing stock of 27 x 10^3 kg Si (1.0 x
537 10^6 mol Si) is obtained (Fig. 4). This figure integrates the seasonal variability occurring over the year
538 cycle in the Bay, which range from a minimal value of 18 x 10^3 kg Si (0.6 x 10^6 mol Si) in winter to a
539 maximum value of 36 x 10^3 kg Si (1.3 x 10^6 mol Si) in spring.

The fate of diatom silica in superficial sediments is largely influenced by the active filter-feeding of mollusks in the Bay, which defecate Si-rich feces that facilitate the retention of diatom silica at the sediment surface (Chauvaud et al. 2000; Ragueneau et al. 2002, 2005). The content of diatom silica in the superficial sediment of the Bay was determined from the analysis of 86 sediment samples from 43 stations across the Bay, which capture both the intra-annual variability (43 samples were sampled in winter and 43 in late summer) and the different depositional environments of the Bay (Song and Ragueneau 2007). It resulted in an average diatom silica reservoir in the superficial sediments of the Bay of 248 x 10^3 kg Si (8.8 x 10^6 mol Si; Fig. 4).

When the Si stocks and fluxes of sponges are compared with those of planktonic diatoms, there are marked differences (Fig. 4). The rates at which Si is processed through diatoms are one order of magnitude higher than those through sponges. On the contrary, diatom Si stocks are between 7 to 45 times smaller than those of sponges (Fig. 4), in agreement with the only study to date comparing Si standing stocks in sponges and diatoms in a coastal ecosystem (Maldonado et al. 2010). These differences indicate that sponges and diatoms play their respective roles in the Si budget of the Bay at different speeds and through different mechanisms. The turnover of the diatom silica standing stock (i.e., standing stock : production rate) in the Bay is about 3 days, whereas that of sponge silica is about 6 years, that is, approximately 800 times slower than that of diatom silica. Similarly, the turnover of diatom silica stock in superficial sediments (i.e., reservoir in sediment : deposition rate) is about 1 month, whereas that of sponge silica is about 16 years (ca. 170 times that of diatom silica). This means that the cycling of Si through diatoms is comparatively faster, with Si mainly cycling through them (repeatedly over a year) rather than being accumulated. In contrast, Si accumulates in huge amounts in sponges over long periods (≥10 y), being slowly processed through them. These results show that impacts on either the sponge populations or the sediments nearby sponge

563 aggregations could have a long-term impact on the sponge Si cycling dynamics, which will require
564 decades to be restored.

565

566 Conclusion

567 In shallow-water ecosystems, planktonic and benthic silicifiers have to share the dSi pool and
568 compete to incorporate this nutrient, which is critical for the growth of both organisms. Our study
569 highlights that even in coastal, shallow-water systems with a high primary productivity dominated by
570 planktonic diatoms —such as the Bay of Brest, sponges may account for a stock of biogenic silica as
571 large as 89-98%. This stock cycles slowly compared to that of diatoms and accumulates bSi in the
572 sediments. These results suggest that the Si cycling through sponge communities is substantially
573 different from that through diatom assemblages. Therefore, the comparison between the roles of these
574 two groups of silicifiers is not straightforward due to their contrasting biological features (e.g.,
575 benthic and long living vs planktonic and short living). Yet these two types of silicifiers need to be
576 quantitatively integrated in future approaches, if we aim to understand in depth the intricacies of the
577 Si cycle in coastal systems.

578

579 Acknowledgments

580 The authors thank Erwan Amice, Isabelle Bihannic, and Thierry Le Bec for assistance during
581 underwater fieldwork and for pictures of Fig. 1b-g. Marta García Puig and Marcos Navas Durán are
582 thanked for helping with the data management of spicule counting. The authors also thank the staff
583 maintaining the Lanvéoc database for making public their information on nutrient availability at the

bottom waters of the Bay of Brest and Sébastien Hervé for the artwork of Fig. 4. Jill Sutton and Fiz Fernández are especially thanked for their comments on the manuscript. This research was supported by two Spanish Ministry grants (CTM2015-67221-R and MICIU: #PID2019-108627RB-I00) to MM, the French National research program EC2CO (grant 12735 – AO2020) to JG, and the ISblue project, Interdisciplinary graduate school for the blue planet (ANR-17-EURE-0015), co-funded by a grant from the French government under the program "Investissements d'Avenir", to MLA. MLA thanks the Xunta de Galicia for her postdoctoral grant (IN606B-2019/002), which also supported this work. The authors declare no conflict of interest.

Author Contributions

MLA and MM conceived and designed the study. MLA conducted the sponge fieldwork, with the help of JG and AL. MLA, MM, and CS taxonomically identified the sponges. MLA processed the sponge samples to determine specific silica content. AH sampled the sediment cores and provided sedimentary data. JG and AH provided the bottom mapping data and MLA developed the benthic habitat and spicule accumulation layers. MLA, CG, and CS conducted sponge silica determination under the microscope. MLA analyzed and interpreted the data and drafted the manuscript, with invaluable inputs made by MM and AL. All authors contributed with comments to the manuscript and approved the submitted version.

References

Armbrust, E. V. 2009. The life of diatoms in the world's oceans. Nature **459**: 185–192. doi:10.1038/nature08057

Ávila, E., and R. Riosmena-Rodriguez. 2011. A preliminary evaluation of shallow-water rhodolith beds in Bahia Magdalena, Mexico. Braz. J. Oceanogr. **59**: 365–375. doi:10.1590/S1679-87592011000400007

Bavestrello, G., R. Cattaneo-Vietti, C. Cerrano, S. Cerutti, and M. Sará. 1996. Contribution of sponge spicules to the composition of biogenic silica in the Ligurian Sea. Mar. Ecol. **17**: 41–50. doi:10.1111/j.1439-0485.1996.tb00488.x

Bell, J. J., A. Biggerstaff, T. Bates, H. Bennett, J. Marlow, E. McGrath, and M. Shaffer. 2017. Sponge monitoring: moving beyond diversity and abundance measures. Ecol. Indic. **78**: 470–488. doi:10.1016/j.ecolind.2017.03.001

Beucher, C., P. Treguer, R. Corvaisier, A. M. Hapette, and M. Elskens. 2004. Production and dissolution of biosilica, and changing microphytoplankton dominance in the Bay of Brest (France). Mar. Ecol. Prog. Ser. **267**: 57–69. doi:10.3354/meps267057

Beudin, A. 2014. Dynamique et échanges sédimentaires en rade de Brest impactés par l'invasion de crépidules. Ph.D. thesis. Université de Bretagne Occidentale.

Chauvaud, L., F. Jean, O. Ragueneau, and G. Thouzeau. 2000. Long-term variation of the Bay of Brest ecosystem: benthic-pelagic coupling revisited. Mar. Ecol. Prog. Ser. **200**: 35–48. doi:10.3354/meps200035

Chou, Y., J. Y. Lou, C.-T. A. Chen, and L.-L. Liu. 2012. Spatial distribution of sponge spicules in sediments around Taiwan and the Sunda Shelf. J. Oceanogr. **68**: 905–912. doi:10.1007/s10872-012-0143-7

626 Chu, J. W. F., M. Maldonado, G. Yahel, and S. P. Leys. 2011. Glass sponge reefs as a silicon sink.
627 Mar. Ecol. Prog. Ser. **441**: 1–14. doi:10.3354/meps09381

628 Davidson, K., R. J. Gowen, P. J. Harrison, L. E. Fleming, P. Hoagland, and G. Moschonas. 2014.
629 Anthropogenic nutrients and harmful algae in coastal waters. J. Environ. Manage. **146**: 206–
630 216. doi:10.1016/j.jenvman.2014.07.002

631 Del Amo, Y., B. Quéguiner, P. Tréguer, H. Breton, and L. Lampert. 1997. Impacts of high-nitrate
632 freshwater inputs on macrotidal ecosystems. II. Specific role of the silicic acid pump in the
633 year-round dominance of diatoms in the Bay of Brest (France). Mar. Ecol. Prog. Ser. **161**:
634 225–237. doi:10.3354/meps161225

635 Delmas, R., and P. Tréguer. 1983. Evolution saisonnière des nutriments dans un écosystème eutrophe
636 de l'Europe Occidentale (la Rade de Brest). Interactions marines et terrestres. Oceanol. Acta
637 **6**: 345–356.

638 Delmas, R., and P. Tréguer. 1985. Simulation de l'évolution de paramètres physiques, chimiques, et
639 de la biomasse phytoplanctonlque en période printanière dans un écosystème littoral
640 macrotidal. Oceanis **11**: 197–211.

641 DeMaster, D. J. 2003. The diagenesis of biogenic silica: chemical transformations occurring in the
642 water column, seabed, and crust, p. 87–98. *In* F.T. Mackenzie [ed.], Treatise on
643 Geochemistry. Elsevier.

644 Derrien-Courtel, S., T. Androuin, E. Ar Gall, and others. 2019. Surveillance du Benthos du littoral
645 Breton. Années 2017-2018 Rapport final. Museum d'Histoire Naturelle de Paris.

646 Eberhardt, L. L. 1978. Appraising variability in population studies. J. Wildlife Manage. **42**: 207.
647 doi:10.2307/3800260

Ehrhold, A., G. Gregoire, S. Sabine, G. Jouet, and P. Le Roy. 2016. Present-day sedimentation rates and evolution since the last maximum flooding surface event in the Bay of Brest (W-N France). Proceedings of the American Geophysical Union, AGU, Fall Meeting 2016.

Ehrhold, A., G. Jouet, P. Le Roy, and others. 2021. Fossil maerl beds as coastal indicators of late Holocene palaeo-environmental evolution in the Bay of Brest (Western France). Palaeogeography, Palaeoclimatology, Palaeoecology **577**: 110525. doi:10.1016/j.palaeo.2021.110525

Erez, J., K. Takahashi, and S. Honjo. 1982. In-situ dissolution experiment of radiolaria in the central North Pacific ocean. Earth Planet. Sci. Lett. **59**: 245–254. doi:10.1016/0012-821X(82)90129-7

Falkowski, P. G., and M. J. Oliver. 2007. Mix and match: how climate selects phytoplankton. Nat. Rev. Microbiol. **5**: 813–819. doi:10.1038/nrmicro1751

Glibert, P. M., and M. A. Burford. 2017. Globally changing nutrient loads and harmful algal blooms. Recent advances, new paradigms, and continuing challenges. Oceanography **30**: 58–69.

Grall, J., and M. Glémarec. 1997. Biodiversity of maerl beds in Brittany: functional approach and anthropogenic impacts. Vie et Milieu **47**: 339–349.

Gregoire, G., A. Ehrhold, P. Le Roy, G. Jouet, and T. Garlan. 2016. Modern morpho-sedimentological patterns in a tide-dominated estuary system: the Bay of Brest (west Britanny, France). J. Maps **12**: 1152–1159. doi:10.1080/17445647.2016.1139514

Gregoire, G., P. Le Roy, A. Ehrhold, G. Jouet, and T. Garlan. 2017. Control factors of Holocene sedimentary infilling in a semi-closed tidal estuarine-like system: the bay of Brest (France). Mar. Geol. **385**: 84–100. doi:10.1016/j.margeo.2016.11.005

Gutt, J., J. Arndt, C. Kraan, B. Dorschel, M. Schröder, A. Bracher, and D. Piepenburg. 2019. Benthic communities and their drivers: a spatial analysis off the Antarctic Peninsula. Limnol. Oceanogr. **64**: 2341–2357. doi:10.1002/lno.11187

Gutt, J., A. Bohmer, and W. Dimmler. 2013. Antarctic sponge spicule mats shape macrobenthic diversity and act as a silicon trap. Mar. Ecol. Prog. Ser. **480**: 57–71. doi:10.3354/meps10226

Hily, C., P. Potin, and J.-Y. Floch. 1992. Structure of subtidal algal assemblages on soft-bottom sediments: fauna/flora interactions and role of disturbances in the Bay of Brest, France. Mar. Ecol. Prog. Ser. **85**: 115–130. doi:10.3354/meps085115

Hooper, J. N. A. 2019. Sponges, p. 170–186. *In* P.A. Hutchings, M. Kingsford, and O. Hoegh-Guldberg [eds.], The Great Barrier Reef: biology, environment and management.

Jean, F. 1994. Modélisation à l'état stable des transferts de carbone dans le réseau trophique benthique de la rade de Brest (France). Ph.D. thesis. Université de Bretagne Occidentale.

Kersken, D., B. Feldmeyer, and D. Janussen. 2016. Sponge communities of the Antarctic Peninsula: influence of environmental variables on species composition and richness. Polar Biol. **39**: 851–862. doi:10.1007/s00300-015-1875-9

Khalil, K., C. Rabouille, M. Gallinari, K. Soetaert, D. J. DeMaster, and O. Ragueneau. 2007. Constraining biogenic silica dissolution in marine sediments: a comparison between diagenetic models and experimental dissolution rates. Mar. Chem. **106**: 223–238. doi:10.1016/j.marchem.2006.12.004

Kristiansen, S., and E. E. Hoell. 2002. The importance of silicon for marine production. Hydrobiologia **484**: 21–31. doi:10.1023/A:1021392618824

Lambert, C., M. Vidal, A. Penaud, N. Combourieu-Nebout, V. Lebreton, O. Ragueneau, and G. Gregoire. 2017. Modern palynological record in the Bay of Brest (NW France): Signal

693 calibration for palaeo-reconstructions. Review of Palaeobotany and Palynology **244**: 13–25.
694 doi:10.1016/j.revpalbo.2017.04.005

695 Le Pape, O., Y. Del Amo, A. Menesguen, A. Aminot, B. Quéquiner, and P. Tréguer. 1996.
696 Resistance of a coastal ecosystem to increasing eutrophic conditions: the Bay of Brest
697 (France), a semi-enclosed zone of Western Europe. Cont. Shelf Res. **16**: 1885–1907.
698 doi:10.1016/0278-4343(95)00068-2

699 López-Acosta, M., A. Leynaert, J. Grall, and M. Maldonado. 2018. Silicon consumption kinetics by
700 marine sponges: an assessment of their role at the ecosystem level. Limnol. Oceanogr. **63**:
701 2508–2522. doi:10.1002/lno.10956

702 López-Acosta, M., A. Leynaert, and M. Maldonado. 2016. Silicon consumption in two shallow-water
703 sponges with contrasting biological features. Limnol. Oceanogr. **61**: 2139–2150.
704 doi:10.1002/lno.10359

705 Lukowiak, M., A. Pisera, and A. O'Dea. 2013. Do spicules in sediments reflect the living sponge
706 community? A test in a Caribbean shallow-water lagoon. PALAIOS **28**: 373–385.
707 doi:10.2110/palo.2012.p12-082r

708 Maldonado, M., R. Aguilar, R. J. Bannister, and others. 2017. Sponge grounds as key marine
709 habitats: a synthetic review of types, structure, functional roles, and conservation concerns, p.
710 145–184. *In* S. Rossi, L. Bramanti, A. Gori, and C. Orejas Saco del Valle [eds.], Marine
711 Animal Forests: The Ecology of Benthic Biodiversity Hotspots. Springer International
712 Publishing.

713 Maldonado, M., L. Beazley, M. López-Acosta, E. Kenchington, B. Casault, U. Hanz, and F. Mienis.
714 2021. Massive silicon utilization facilitated by a benthic-pelagic coupled feedback sustains
715 deep-sea sponge aggregations. Limnol Oceanogr **66**: 366–391. doi:10.1002/lno.11610

716 Maldonado, M., C. Carmona, Z. Velásquez, A. Puig, A. Cruzado, A. López, and C. M. Young. 2005.
717 Siliceous sponges as a silicon sink: an overlooked aspect of benthopelagic coupling in the
718 marine silicon cycle. Limnol. Oceanogr. **50**: 799–809. doi:10.4319/lo.2005.50.3.0799

719 Maldonado, M., M. López-Acosta, L. Beazley, E. Kenchington, V. Koutsouveli, and A. Riesgo.
720 2020. Cooperation between passive and active silicon transporters clarifies the ecophysiology
721 and evolution of biosilicification in sponges. Sci. Adv. **6**: eaba9322.
722 doi:10.1126/sciadv.aba9322

723 Maldonado, M., M. López-Acosta, C. Sitjà, M. García-Puig, C. Galobart, G. Ercilla, and A. Leynaert.
724 2019. Sponge skeletons as an important sink of silicon in the global oceans. Nat. Geosci. **12**:
725 815–822. doi:10.1038/s41561-019-0430-7

726 Maldonado, M., L. Navarro, A. Grasa, A. González, and I. Vaquerizo. 2011. Silicon uptake by
727 sponges: a twist to understanding nutrient cycling on continental margins. Sci Rep **1**: 8.
728 doi:10.1038/srep00030

729 Maldonado, M., A. Riesgo, A. Bucci, and K. Rützler. 2010. Revisiting silicon budgets at a tropical
730 continental shelf: silica standing stocks in sponges surpass those in diatoms. Limnol.
731 Oceanogr. **55**: 2001–2010. doi:10.4319/lo.2010.55.5.2001

732 Malviya, S., E. Scalco, S. Audic, and others. 2016. Insights into global diatom distribution and
733 diversity in the world's ocean. Proc Natl Acad Sci USA **113**: E1516–E1525.
734 doi:10.1073/pnas.1509523113

735 McGrath, E. C., L. Woods, J. Jompa, A. Haris, and J. J. Bell. 2018. Growth and longevity in giant
736 barrel sponges: redwoods of the reef or pines in the Indo-Pacific? Sci Rep **8**: 15317.
737 doi:10.1038/s41598-018-33294-1

McMurray, S. E., J. E. Blum, and J. R. Pawlik. 2008. Redwood of the reef: growth and age of the giant barrel sponge *Xestospongia muta* in the Florida Keys. Mar. Biol. **155**: 159–171. doi:10.1007/s00227-008-1014-z

McMurray, S. E., C. M. Finelli, and J. R. Pawlik. 2015. Population dynamics of giant barrel sponges on Florida coral reefs. J. Exp. Mar. Biol. Ecol. **473**: 73–80. doi:10.1016/j.jembe.2015.08.007

Neill, K. F., W. A. Nelson, R. D'Archino, D. Leduc, and T. J. Farr. 2015. Northern New Zealand rhodoliths: assessing faunal and floral diversity in physically contrasting beds. Mar Biodiv **45**: 63–75. doi:10.1007/s12526-014-0229-0

Ng, H. C., L. Cassarino, R. A. Pickering, E. M. S. Woodward, S. J. Hammond, and K. R. Hendry. 2020. Sediment efflux of silicon on the Greenland margin and implications for the marine silicon cycle. Earth Planet. Sci. Lett. **529**: 115877. doi:10.1016/j.epsl.2019.115877

QGIS Development Team. 2020. QGIS Geographic Information System, Open Source Geospatial Foundation Project.

Quéguiner, B., and P. Tréguer. 1984. Studies on the phytoplankton in the bay of Brest (western Europe). Seasonal variations in composition, biomass and production in relation to hydrological and chemical features (1981-1982). Bot. Mar. **27**: 449–459. doi:10.1515/botm.1984.27.10.449

Ragueneau, O., L. Chauvaud, A. Leynaert, and others. 2002. Direct evidence of a biologically active coastal silicate pump: ecological implications. Limnol. Oceanogr. **47**: 1849–1854. doi:10.4319/lo.2002.47.6.1849

Ragueneau, O., L. Chauvaud, B. Moriceau, A. Leynaert, G. Thouzeau, A. Donval, F. Le Loc'h, and F. Jean. 2005. Biodeposition by an invasive suspension feeder impacts the biogeochemical

cycle of Si in a coastal ecosystem (Bay of Brest, France). Biogeochemistry **75**: 19–41. doi:10.1007/s10533-004-5677-3

Ragueneau, O., D. J. Conley, A. Leynaert, S. N. Longphuirt, and C. P. Slomp. 2006. Role of diatoms in silica cycling and coastal marine food webs, p. 163–195. *In* V. Ittekkot, D. Unger, C. Humborg, and N.T. An [eds.], The silicon cycle: human perturbations and impacts on aquatic systems. Island Press.

Ragueneau, O., M. Raimonet, C. Mazé, and others. 2018. The impossible sustainability of the Bay of Brest? Fifty years of ecosystem changes, interdisciplinary knowledge construction and key questions at the science-policy-community interface. Front. Mar. Sci. **5**: 124. doi:10.3389/fmars.2018.00124

Raimonet, M., O. Ragueneau, F. Andrieux-Loyer, X. Philippon, R. Kerouel, M. Le Goff, and L. Mémery. 2013. Spatio-temporal variability in benthic silica cycling in two macrotidal estuaries: Causes and consequences for local to global studies. Estuar. Coast. Shelf Sci. **119**: 31–43. doi:10.1016/j.ecss.2012.12.008

Reincke, T., and D. Barthel. 1997. Silica uptake kinetics of *Halichondria panicea* in Kiel Bight. Marine Biology **129**: 591–593. doi:10.1007/s002270050200

Rickert, D., M. Schlüter, and K. Wallmann. 2002. Dissolution kinetics of biogenic silica from the water column to the sediments. Geochim. Cosmochim. Acta **66**: 439–455. doi:10.1016/S0016-7037(01)00757-8

Ríos, P., and J. Cristobo. 2014. Antarctic Porifera database from the Spanish benthic expeditions. ZooKeys **401**: 1–10. doi:10.3897/zookeys.401.5522

Rützler, K., and I. G. Macintyre. 1978. Siliceous sponge spicules in coral-reef sediments. Mar. Biol. **49**: 147–159. doi:10.1007/bf00387114

783 Salomon, J. C., and M. Breton. 1991. Numerical study of the dispersive capacity of the Bay of Brest,
784 France, towards dissolved substances, p. 459–464. *In* Environmental hydraulics.

785 Sandford, F. 2003. Physical and chemical analysis of the siliceous skeletons in six sponges of two
786 groups (Demospongiae and Hexactinellida). Microsc. Res. Tech. **62**: 336–355.
787 doi:10.1002/jemt.10400

788 Sañé, E., E. Isla, M. Á. Bárcena, and D. J. DeMaster. 2013. A shift in the biogenic silica of sediment
789 in the Larsen B continental shelf, off the Eastern Antarctic Peninsula, resulting from climate
790 change V. Magar [ed.]. PLoS ONE **8**: e52632. doi:10.1371/journal.pone.0052632

791 Sarmiento, J., and N. Gruber. 2006. Ocean biogeochemical dynamics, Princeton University Press.

792 Sarthou, G., K. R. Timmermans, S. Blain, and P. Tréguer. 2005. Growth physiology and fate of
793 diatoms in the ocean: a review. J. Sea Res. **53**: 25–42. doi:10.1016/j.seares.2004.01.007

794 Sciberras, M., M. Rizzo, J. R. Mifsud, K. Camilleri, J. A. Borg, E. Lanfranco, and P. J. Schembri.
795 2009. Habitat structure and biological characteristics of a maerl bed off the northeastern coast
796 of the Maltese Islands (central Mediterranean). Mar. Biodiv. **39**: 251–264.
797 doi:10.1007/s12526-009-0017-4

798 Song, Y. P., and O. Ragueneau. 2007. Le dosage de bSiO2 dans le sédiment de la rade de Brest.
799 Master thesis. Université de Bretagne Occidentale.

800 Teixidó, N., J. Garrabou, and J.-G. Harmelin. 2011. Low dynamics, high longevity and persistence of
801 sessile structural species dwelling on Mediterranean coralligenous outcrops S. Thrush [ed.].
802 PLoS ONE **6**: e23744. doi:10.1371/journal.pone.0023744

803 Thorel, M., P. Claquin, M. Schapira, and others. 2017. Nutrient ratios influence variability in
804 *Pseudo-nitzschia* species diversity and particulate domoic acid production in the Bay of Seine
805 (France). Harmful Algae **68**: 192–205. doi:10.1016/j.hal.2017.07.005

806 Tréguer, P. J., J. N. Sutton, M. Brzezinski, and others. 2021. Reviews and syntheses: The
807 biogeochemical cycle of silicon in the modern ocean. Biogeosciences **18**: 1269–1289.
808 doi:10.5194/bg-18-1269-2021

809 Van Soest, R. W. M., N. Boury-Esnault, J. Vacelet, and others. 2012. Global diversity of sponges
810 (Porifera). PLOS ONE **7**: e35105. doi:10.1371/journal.pone.0035105

811

Table 3. Summary of biogenic silica (bSi) standing stock in the sponge assemblages of the Bay of Brest (France). Average (±SD) silica content per unit of volume of living sponge tissue (mg bSi mL^{-1}) of each siliceous sponge species and average (±SD) sponge Si stock per square meter (mg Si m^{-2}) in each habitat (RI, rocky intertidal; RS, rocky subtidal; MB, maerl beds; SM, shallow mud; HS, heterogeneous sediments; CS, circalittoral coarse sediments) and for the total ecosystem of the Bay of Brest.

	BSi content		Sponge contribution to the BSi standing stock (mg Si m^{-2})											
	(mg BSi mL^{-1})		RI		RS		MB		SM		HS		CS	
Sponge species	Mean	SD	Mean	SD	Mean	SD	Mean	SD	Mean	SD	Mean	SD	Mean	SD
Amphilectus fucorum	36.13	4.79			222.88	655.79	27.59	124.16			3.17	13.25	5.31	25.44
Antho inconstans	33.27	4.25			101.84	567.05								
Biemna variantia	45.38	4.86			4.79	26.67								
Bubaris vermiculata	96.21	11.21											6.77	24.33
Chalinula cf. *limbata*	43.92	6.96			31.79	177.00								
Ciocalypta penicillus	103.61	0.39			374.14	1,456.86								
Clathria strepsitoxa	29.78	2.89			194.81	519.89					0.77	4.64	0.76	2.39
Cliona celata	85.58	7.24			134,576.89	389,757.49			2,961.26	11,145.37	1.11	6.67	64.09	134.54
Cliona lobata	78.15	5.94											102.10	122.41
Halichondria bowerbanki	58.33	1.83			7.92	32.41	116.13	724.07					0.28	0.96
Halichondria panicea	55.40	11.30	134.18	337.69	60.07	197.04	268.83	677.52			1.56	4.75	3.97	14.96
Halichondria sp.	71.38	0.77			434.84	949.91	73.18	336.72						
Haliclona angulata	39.55	6.92											25.17	69.19
Haliclona cinerea	37.79	4.50			17.10	95.19	6.91	18.02			1.16	6.94	1.48	3.37
Haliclona fibulata	53.64	6.23											132.65	386.64
Haliclona fistulosa	52.52	21.55			24.29	135.26	18.65	116.43					11.64	55.80
Haliclona rosea	32.94	5.41			13.16	45.12	116.88	253.13			20.32	115.42	1.97	6.53
Haliclona simulans	74.95	16.47			554.65	1,613.25	613.86	1,374.11			152.11	411.44	57.56	150.02
Hemimycale columella	49.41	7.03			621.31	1,625.25	37.82	165.58			8.66	51.97	1.10	5.27

Hymedesmia cf. *occulta*	35.99	6.52											0.88	3.20
Hymedesmia coriacea	32.58	6.30			0.49	2.74	5.81	27.81					0.65	3.11
Hymedesmia jecusculum	36.29	5.67			21.73	86.53								
Hymedesmia lenta	30.47	5.05)			7.75	43.17							7.48	27.56
Hymeniacidon perlevis	48.88	6.18	1,975.23	2,898.50	794.85	1,854.75	3,968.75	5,403.69			596.50	1,273.29	54.60	248.94
Iophon hyndmani	42.56	3.16											5.36	16.97
Iophon nigricans	43.77	2.11											200.99	905.76
Mycale contarenii	62.69	7.71			86.50	222.88	20.88	91.83			117.22	594.43		
Mycale macilenta	52.87	5.32			795.91	2,050.78	0.14	0.88			16.91	69.90	3.19	8.36
Myxilla fimbriata	50.77	4.34			128.62	340.78							0.39	1.86
Myxilla rosacea	42.64	4.02											0.15	0.73
Pachymatisma johnstonia	116.70	22.01			3,918.18	15,445.96								
Paratimea constellata	66.94	4.07											0.44	1.83
Phorbas fictitius	93.20	5.22			420.82	2,061.94	497.65	1,419.77						
Phorbas plumosus	40.95	15.92			122.27	649.18	52.54	160.68						
Polymastia boletiformis	58.91	11.51			58.63	326.44							0.29	1.38
Polymastia penicillus	71.41	7.84	1.27	6.09	230.17	1,258.52							0.10	0.46
Protosuberites cf. *denhartogi*	57.84	4.85			77.23	287.25					0.56	3.38		
Raspailia ramosa	56.76	5.60											1.69	8.12
Spanioplon armaturum	32.48	3.26			463.15	920.96							0.24	0.96
Stelligera stuposa	44.70	3.04			76.69	238.29					0.58	3.48	0.74	3.48
Suberites ficus	114.77	12.45					995.23	6,105.84	582.80	1,801.65	4,972.06	20,926.78		
Suberites massa	96.02	4.70					0.25	1.60						
Tedania anhelans	34.90	6.42					105.64	493.25					122.48	266.90
Tethya citrina	145.57	14.17	2,166.28	3,780.43	5,623.00	15,889.11	3,103.96	5,192.50			1,743.08	3,022.67	76.76	150.91
Timea crassa	93.89	4.14									101.31	449.00	161.92	608.25
Total	59.61	27.07	4,283.08	4,191.32	151,079.97	387,576.21	10,035.84	10,742.40	3,544.06	11,126.45	7,737.09	20,560.60	794.06	1,392.12

816

Supplemental Information

Supplementary Table 1. Average concentration (±SD) of dissolved silicon (µmol Si L^{-1}) at the bottom waters of the Bay of Brest. Data come from the Lanvéoc long-term survey series (48.295777° N, 4.454758° W), which sampled bottom water with a 1L syringe manually by scientific divers just over seabed every two weeks at high tide. Data integrated dissolved silicon concentrations from the last decade (2012-2021).

	Dissolved Si concentration	
Month	**AVRG**	**SD**
Jan	11.03	2.79
Feb	13.28	5.68
Mar	8.89	5.77
Apr	2.44	2.20
May	3.60	4.25
Jun	2.44	1.22
Jul	2.10	0.93
Aug	2.83	0.55
Sep	4.85	2.20
Oct	8.35	5.08
Nov	8.57	2.46
Dec	10.13	2.36

Supplementary Table 2. List of the sponge species of the Bay of Brest (France). Presence at each habitat is indicated. RI, rocky intertidal; RS, rocky subtidal; MB, maerl beds; SM, shallow mud; HS, heterogeneous sediments; CS, circalittoral coarse sediments.

	Habitat					
	RI	**RS**	**MB**	**SM**	**HS**	**CS**
Class DEMOSPONGIAE						
Subclass HETEROSCLEROMORPHA						
Order AXINELLIDA						
Family RASPAILIIDAE						
Raspailia ramosa						X
Family STELLIGERIDAE						
Paratimea constellata						X
Stelligera stuposa		X			X	X
Order BIEMNIDA						
Family BIEMNIDAE						
Biemna variantia		X				
Order BUBARIDA						
Family BUBARIDAE						
Bubaris vermiculata						X
Order CLIONAIDA						
Family CLIONAIDAE						
Cliona celata		X		X	X	X
Cliona lobata						X
Order HAPLOSCLERIDA						
Family CHALINIDAE						
Chalinula cf. *limbata*		X				
Haliclona angulata						X
Haliclona cinerea		X	X		X	X
Haliclona fibulata						X
Haliclona fistulosa		X	X			X
Haliclona rosea		X	X		X	X
Haliclona simulans		X	X		X	X
Order POECILOSCLERIDA						
Family ACARNIDAE						
Iophon hyndmani						X
Iophon nigricans						X
Family ESPERIOPSIDAE						
Amphilectus fucorum		X	X		X	X

Table S2. (Continued)

	Habitat					
	RI	**RS**	**MB**	**SM**	**HS**	**CS**
Family HYMEDESMIIDAE						
Hemimycale columella		X	X		X	X
Hymedesmia cf. *occulta*						X
Hymedesmia coriacea		X	X			X
Hymedesmia jecusculum		X				
Hymedesmia lenta		X				X
Phorbas fictitius		X	X			
Phorbas plumosus		X	X			
Spanioplon armaturum		X				X
Family MICROCIONIDAE						
Antho inconstans		X				
Clathria strepsitoxa		X			X	X
Family MYCALIDAE						
Mycale contarenii		X	X		X	
Mycale macilenta		X	X		X	X
Family MYXILLIDAE						
Myxilla fimbriata		X				X
Myxilla rosacea						X
Family TEDANIIDAE						
Tedania anhelans			X			X
Order POLYMASTIIDA						
Family POLYMASTIIDAE						
Polymastia boletiformis		X				X
Polymastia penicillus	X	X				X
Order SUBERITIDA						
Family HALICHONDRIIDAE						
Ciocalypta penicillus		X				
Halichondria bowerbanki		X	X			X
Halichondria panicea	X	X	X		X	X
Halichondria sp.		X	X			
Hymeniacidon perlevis	X	X	X		X	X
Family SUBERITIDAE						
Protosuberites cf. *denhartogi*		X			X	
Suberites ficus			X	X	X	
Suberites massa			X			

Table S2. (Continued)

	Habitat					
	RI	**RS**	**MB**	**SM**	**HS**	**CS**
Order TETHYIDA						
Family TETHYIDAE						
Tethya citrina	X	X	X		X	X
Family TIMEIDAE						
Timea crassa					X	X
Order TETRACTINELLIDA						
Family GEODIIDAE						
Pachymatisma johnstonia		X				
Subclass KERATOSA						
Order DENDROCERATIDA						
Family DARWINELLIDAE						
Aplysilla rosea		X	X		X	
Aplysilla sulfurea		X	X			
Order DICTYOCERATIDA						
Family DYSIDEIDAE						
Dysidea fragilis		X	X			
Family THORECTIDAE						
Hyrtios sp.			X			
Order DENDROCERATIDA						
Family DICTYODENDRILLIDAE						
Spongionella cf. *pulchella*		X				
Subclass VERONGIMORPHA						
Order CHONDRILLIDA						
Family HALISARCIDAE						
Halisarca dujardinii						X
Class CALCAREA						
Subclass CALCARONEA						
Order LEUCOSOLENIDA						
Family SYCETTIDAE						
Sycon ciliatum		X	X			
Subclass CALCINEA						
Order CLATHRINIDA						
Family CLATHRINIDAE						
Clathrina cf. *coriacea*			X			